Contribution from the Chemistry Department,
York University, North York, Ontario, Canada M3J 1P3

Surface Electrochemistry of Chloro(phthalocyaninato)rhodium(III) Species and Oxygen Reduction Electrocatalysis. Formation of a Dimeric Species

Yu-Hong Tse, Penny Seymour, Nagao Kobayashi,[1] Herman Lam, Clifford C. Leznoff, and A. B. P. Lever*

Received November 27, 1990

The deposition of chloro(phthalocyaninato)rhodium(III) onto a highly oriented pyrolytic graphite (HOPG) electrode leads to a surface which can be organized by polarizing to potentials negative of the reduction of rhodium(III) to rhodium(II). The organized surface contains dinuclear rhodium phthalocyanine, which is fairly stable in its $[Rh^{II}Pc]_2$ oxidation state. It is reversibly oxidized to a $[Rh^{III}Pc]_2$ dinuclear species, which decomposes slowly to monomeric $Rh^{III}Pc$, detected upon the surface through its electroactivity. Reduction of mononuclear $Rh^{III}Pc$ back to $Rh^{II}Pc$ leads to redimerization. The surface electrochemistry of this dynamic interplay between mononuclear and dinuclear species is explored in depth. The dinuclear $[Rh^{II}Pc]_2$ species reacts with oxygen to form oxygen adducts, which appear to be involved in both the 2-electron reduction of oxygen to hydrogen peroxide and the 4-electron reduction to water. However, these two processes proved difficult to characterize.

Introduction

Many cobalt and iron MN_4 macrocyclic complexes catalyze the electroreduction of oxygen.[2-8] Most mononuclear cobalt macrocycles catalyze the 2-electron reduction to hydrogen peroxide, but some dinuclear cobalt complexes catalyze the much more desirable 4-electron reduction to water in strongly acidic[9,10] or basic[11] media. Iron porphyrins[2-8] and a dinuclear iridium porphyrin[12] generally catalyze the 4-electron process. Among the phthalocyanines, the iron[13-16] and platinum[17] species are active, in alkaline media, in the 4-electron reduction of oxygen. There are reports of a catena-CN-bridged $Co^{III}Pc$[18] and a mononuclear long-chain ring-substituted cobalt(II) phthalocyanine[19] being active in the 4-electron reduction of oxygen. However, there is no detailed understanding of the role of pH nor indeed of the structural design aspects which favor the 4-electron process over the 2-electron process.

Although the cobalt macrocycles catalyze the 2-electron reduction of oxygen, the existence of the iridium species catalyzing the direct 4-electron process raises the question of whether rhodium macrocycles would be capable of 4-electron reduction, either in a mononuclear form analogous to iron phthalocyanine or in a dinuclear form analogous to the iridium porphyrin.[12] We describe here results obtained with chlororhodium(III) phthalocyanine (**1**)[20,21] adsorbed on highly oriented pyrolytic graphite (HOPG). Evidence for both a 2-electron and a 4-electron reduction was obtained, but we were unsuccessful in determining precisely the conditions which would favor one mechanism over the other.

Nevertheless, in pursuing this investigation, some very interesting surface electrochemical characteristics were observed. The weakly aggregated species attach to the electrode in an irregular fashion, giving a poorly organized surface. Reduction to rhodium(II) phthalocyanine leads to a dimerization process, and electrochemically cycling the electrode converts the poorly organized surface into a simple surface containing almost solely a dimeric rhodium phthalocyanine species.

This paper reports the stability, redox chemistry, and oxygen reduction chemistry of this dimer surface.

Experimental Section

Materials. Tetrabutylammonium perchlorate (TBAP, Aldrich) recrystallized from absolute ethanol was dried in a vacuum oven at 50 °C for 48 h. 1,2-Dichlorobenzene (DCB, Aldrich) and dimethylformamide (DMF, Aldrich) were used as supplied. Argon gas (Linde) was purified by passage through heated copper filings, anhydrous $CaSO_4$ (Drierite), molecular sieves (BDH 3A), and glass wool. Oxygen gas (Linde) was used as received.

Buffer solutions were prepared from 0.1 M solutions of reagent grade H_3PO_4, KH_2PO_4, K_2HPO_4, and KOH and adjusted to the desired pH and approximately constant ionic strength. Distilled water for buffer solutions was doubly distilled in glass from alkaline $KMnO_4$ and then passed through a Barnstead organic removal cartridge and two Barnstead mixed-resin ultrapure cartridges. Buffer solutions were saturated with argon or oxygen for about 1 h and maintained under an atmosphere of the appropriate gas during data collection. Oxygenated solutions contained an oxygen concentration of approximately 10^{-3} M.

Physical Measurements. Electronic spectra were recorded with a Hitachi Perkin-Elmer Model 340 microprocessor spectrometer or a Guided Wave Inc. Model 100-20 optical waveguide spectrum analyzer with a WW100 fiber optic probe. FTIR spectra were obtained as Nujol mulls using a Nicolet SX20 instrument.

Solution electrochemical data were obtained with a Princeton Applied Research (PARC) Model 174 potentiostat or a PARC Model 173 polarographic analyzer, coupled to a PARC Model 175 universal programmer. Cyclic voltammetry and differential-pulse voltammetry (DPV), carried out under an atmosphere of argon, used a conventional three-electrode cell. The working electrode, described by the cross-sectional area of a 27-gauge platinum wire (area 10^{-3} cm^2), was sealed in glass. A platinum wire also served as the counter electrode. The reference electrode was a silver-wire quasi-electrode separated from the working compartment by a glass frit. The potentials were referenced internally to the ferrocenium/ferrocene (Fc^+/Fc) couple (+0.40 V vs SCE, in DMF).

Electrochemical studies of the surface species were performed with a Pine Instrument RDE-3 potentiostat, and the rotating studies, with a Pine Instrument PIR rotator. The working-electrode material for both surface electrochemical and oxygen reduction studies was highly oriented pyrolytic graphite (HOPG) having a circular area of 0.495 cm^2. Before each experiment, the HOPG electrode surface was cleaned by removing sev-

(1) Visiting Professor from the Pharmaceutical Institute, Tohoku University, Sendai 980, Japan.
(2) Jahnke, H.; Schonborn, M.; Zimmermann, G. *Top. Curr. Chem.* **1976**, *61*, 133.
(3) Tarasevich, M. R.; Radyushkina, K. A. *Russ. Chem. Rev.* (*Engl. Transl.*) **1980**, *49*, 1498.
(4) van den Brink, F.; Barendrecht, E.; Visscher, W. *Recl. Trav. Chim. Pays-Bas* **1980**, *99*, 253.
(5) vanVeen, J. A. R.; van Baar, J. F. *Rev. Inorg. Chem.* **1982**, *4*, 293.
(6) Schiffrin, D. J. *Electrochemistry* **1983**, *8*, 126.
(7) Yeager, E. *Electrochim. Acta* **1984**, *29*, 1527. Yeager, E. *J. Mol. Catal.* **1986**, *38*, 5.
(8) Coowar, F.; Contamin, O.; Savy, M.; Scarbeck, G. *J. Electroanal. Chem. Interfacial Electrochem.* **1988**, *246*, 119.
(9) Collman, J. P.; Marrocco, M.; Denisevich, P.; Koval, C.; Anson, F. C. *J. Electroanal. Chem. Interfacial Electrochem.* **1979**, *101*, 117. Collman, J. P.; Denisevich, P.; Konai, Y.; Marrocco, M.; Koval, C.; Anson, F. C. *J. Am. Chem. Soc.* **1980**, *102*, 6027.
(10) Chang, C. K.; Liu, H. Y.; Abdalmuhdi, I. *J. Am. Chem. Soc.* **1984**, *106*, 2725.
(11) van der Putten, A.; Elzing, A.; Visscher, W.; Barendrecht, E. *J. Chem. Soc., Chem. Commun.* **1986**, 477.
(12) Collman, J. P.; Kim, A. *J. Am. Chem. Soc.* **1986**, *108*, 7847.
(13) Kozawa, A.; Zilionis, V. E.; Brodd, R. J. *J. Electrochem. Soc.* **1970**, *117*, 1470.
(14) Kozawa, A.; Zilionis, V. E.; Brodd, R. J. *J. Electrochem. Soc.* **1971**, *118*, 1705.
(15) Zagal, J.; Bindra, P.; Yeager, E. *J. Electrochem. Soc.* **1980**, *127*, 1506.
(16) Kobayashi, N.; Nishiyama, Y. *J. Phys. Chem.* **1985**, *89*, 1167.
(17) Paliteiro, C.; Hamnett, A.; Goodenough, J. *J. Electroanal. Chem. Interfacial Electrochem.* **1984**, *160*, 359.
(18) Ikeda, O.; Itoh, S.; Yoneyama, H. *Bull. Chem. Soc. Jpn.* **1988**, *61*, 1428.
(19) Kobayashi, N.; Sudo, K.; Osa, T. *Bull. Chem. Soc. Jpn.* **1990**, *63*, 571.
(20) Muenz, X.; Hanack, M. *Chem. Ber.* **1988**, *121*, 235.
(21) Berezin, B. D. *Dokl. Akad. Nauk SSSR* **1963**, *150*, 1039.

0020-1669/91/1330-4453$02.50/0

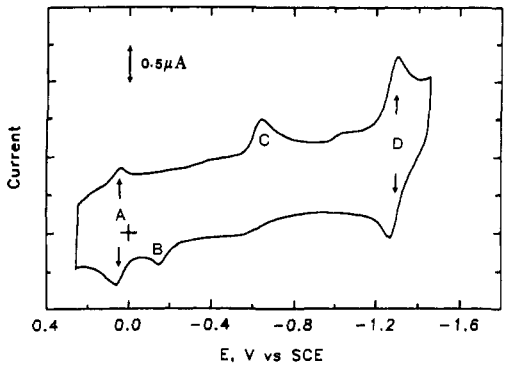

Figure 1. Solution electrochemical cyclic voltammogram for $ClRh^{III}Pc$ (**1**) in DMF (0.1 M TBAP) (platinum working electrode; scan rate 200 mV/s). In all CV scans reported in the figures, cathodic current (reduction) is uppermost.

eral layers of the surface with a transparent adhesive tape. For the adsorption of the catalysts onto the HOPG surface, the electrode was immersed in a (1–5) × 10^{-5} M phthalocyanine solution in DCB, containing about 5% ethanol, for ca. 15 min, removed from the solution, and washed with ethanol and distilled water. The cell comprised a separate chamber for each electrode, with a Luggin capillary extending from the reference chamber to the proximity of the HOPG surface. For the aqueous experiments, an SCE and a large platinum plate were used as a reference and a counter electrode, respectively. For collection of rigorously oxygen-free data, the catalyst adsorption and its study were performed with equipment inside a Vacuum Atmospheres controlled-atmosphere box.

A bulk solution containing dimeric $[Rh^{II}Pc]_2$ was prepared by polarizing a DMF solution of $ClRh^{III}Pc$ (2 × 10^{-4} M; 0.2 M TBAP) at −0.9 V vs AgCl/Ag for 3 h. This solution, maintained in a Vacuum Atmospheres drybox, was used to deposit the dimeric species directly upon a prepared HOPG electrode; deposition time was 0.5–1.0 h.

Chloro(phthalocyaninato)rhodium(III) (1) ($ClRh^{III}Pc$). $ClRh^{III}Pc$ was prepared from $RhCl_3 \cdot 2H_2O$, phthalonitrile, and urea, using the melt method.[22] The melt solidified after 15 min of heating over an open flame and was cooled to ambient temperature, whereupon the fused solid was broken down by boiling with ethanol. The ethanol was boiled off, and the solid crude $ClRh^{III}Pc$ (plus unreacted starting materials and impurities) was sequentially extracted with benzene for 41 h, with acetone for 48 h, and with pyridine for 2 h. The solid recovered from the pyridine extract was further extracted with CH_2Cl_2 for 15–20 hours and dissolved in DMF, and the solution was poured into cold dilute HCl. The resulting precipitate was subsequently boiled with 1 M HCl, filtered out, washed with 0.1 M HCl, and finally dried in vacuo at 100 °C for 7 h. Anal. Calc: C, 59.05; H, 2.47; N, 17.21. Found: C, 58.72; H, 2.70; N, 17.09. FTIR: 1523 s, 1502 m, 1331 m, 1287 m, 1169 m, 1122 s, 1066 m, 913 m, 777 w, 757 m, 729 s, 574 w cm^{-1}. UV/vis (λ_{max}, nm (log ϵ)): 342 (4.45), 598 (4.46), 665 (5.15), in DCB. Similar data for $ClRh^{III}Pc$ dissolved in chloroform have been reported.[20]

Chloro(tetraneopentoxyphthalocyaninato)rhodium(III) (2) (ClRhTNPc). 4-Neopentoxyphthalonitrile (1.28 g, 6 mmol) and $Rh_2(CO)_2Cl_2$ (0.25 g, 0.75 mmol) were heated in (dimethylamino)ethanol (25 mL) at 165 °C for 48 h. The crude reaction mixture was poured into water, and the resulting precipitate was filtered out, washed, and dried overnight to yield 1.5 g of crude green solid. This solid was preabsorbed onto flash silica gel and eluted with 1:1 hexane/chloroform to give, upon evaporation, a bluish green solid. Yield: 0.12 g (7%) of dark blue shining crystals. Anal. Calc for $ClRhTNPc \cdot C_6H_{14}$: C, 64.41; H, 6.52; N, 10.36. Found: C, 64.6; H, 6.0; N, 10.0. FTIR: 2955 s, 2868 s, 1611 s, 1508 m, 1488 m, 1457 w, 1397 s, 1385 s, 1285 w, 1237 s, 1129 s, 1111 s, 1061 s, 1013 m, 826 w, 753 w cm^{-1}. These data are very similar to those reported for a series of divalent MTNPc derivatives.[23] UV/vis (λ_{max}, nm (log ϵ)) 349 (4.48), 594 (4.43), 657 (5.21), in DCB.

Results

(i) Solution Electrochemistry. The cyclic voltammogram of $ClRh^{III}Pc$ in DMF solution (Figure 1) shows three major features: a reversible couple, A, at +0.05 V vs SCE; two widely separated peaks at −0.15 V (anodic), B and −0.65 V (cathodic), C; and another reversible couple, D, near −1.4 V vs. SCE. Couples A and B were generated only by polarizing the electrode negative of peak C. If the solution is cooled to about −72 °C, peak C becomes reversible, peak B disappears, and peak A is replaced by a small irreversible anodic peak at 0.32 V. A spectroelectrochemical study of the bulk reduced species, obtained by reduction ~100 mV negative of peak C, produces the spectra shown in Figure 2. The solution electrochemistry has been studied as a function of solvent, temperature, and supporting electrolyte. The salient features are reported in the Discussion, but the details will appear elsewhere.[24]

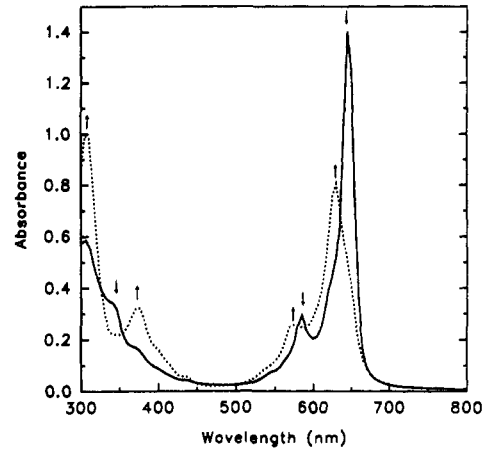

Figure 2. Spectroelectrochemical study of the reduction of $ClRh^{III}Pc$ (**1**) in DMF. For details see text.

(ii) Surface Electrochemistry. *Drybox or argon conditions*: It is necessary to distinguish carefully two sets of conditions used for studying the surface electrochemistry. In one set, drybox conditions were used to exclude all traces of oxygen. In the other set, an argon-degassed cell was employed in the open laboratory to obtain the initial "oxygen-free" conditions prior to saturating the cell with oxygen to study oxygen electrocatalysis. These "oxygen-free" conditions in degassed argon do in fact contain traces of oxygen, which it proved impossible to absolutely exclude without using a controlled-atmosphere box (drybox).

We have studied both the unsubstituted phthalocyanine species $ClRh^{III}Pc$ (**1**) and $ClRh^{III}TNPc$ (**2**) (TNPc = tetraneopentoxyphthalocyanine, being a mixture of isomers having one neopentoxy group in a peripheral position in each of the benzene rings). The results are described for both systems without differentiation except where such distinction is relevant.

In both the drybox and argon-degassed experiments, the first-scan cyclic voltammogram of a freshly prepared chloro(phthalocyaninato)rhodium-modified HOPG electrode run negatively from about 0.3 V shows no peak near 0 V but does have rapidly rising cathodic current more negative than about −0.5 V for **1** and more negative than about −0.6 V for **2**, with a more prominent peak at about −0.9 to −1.0 V for species **1** and nearer −0.8 V for species **2** (labeled peak V below) (Figure 3A,B). If this scan is extended, negatively, beyond the peak at about −0.8 V and then switched, there is a decline in the cathodic current in the −0.5 to −1.0 V region, a dramatic loss of current in peak V, and the buildup of a new reversible peak near 0 V (peak I) (+0.03 V for ClRhPc and −0.05 V vs SCE for ClRhTNPc, at pH 12.9), during the second and subsequent scans. Peak I builds up rapidly if multiple scans are switched near −1.0 to −1.2 V. It is just barely observable if a freshly deposited surface is switched at −0.6 V. Such scans reach an equilibrium when the current of peak I ceases to increase with subsequent scans. Species **1** and **2** behave analogously except that equilibrium formation of peak I is much more facile for species **2**, being almost complete by the second scan (Figure 3A).

Peak I is most clearly observed in basic medium. As the pH decreases, the half-peak potential for couple I shifts positive with

(22) Keen, I. M.; Malerbi, B. W. *J. Inorg. Nucl. Chem.* **1965**, *27*, 1311.
(23) Fu, G.; Fu, Y.-S.; Jayaraj, K.; Lever, A. B. P. *Inorg. Chem.* **1990**, *29*, 4090.
(24) Manivannan, V.; Persaud, L.; Tse, Y.-H.; Kobayashi, N.; Lever, A. B. P. Paper in preparation.

Table I. Peak Potentials (V vs SCE) of Peak I as a Function of pH[a]

pH	E(peak I)[b]	pH	E(peak I)[b]	pH	E(peak I)[b]
9.2	+0.16	10.8	+0.08	12.7	+0.03
9.75	+0.11	11.4	+0.09	12.8	+0.02
9.8	+0.11	12.4	+0.03	12.9	+0.01

[a] In general, peak I was very poorly defined at acid pH. [b] The average of the anodic and cathodic components is cited. These occurred at the same potential or close thereto. The equation of the best line is (peak I) $E = -[0.034\ (0.003)]\text{pH} + [0.45\ (0.01)]$ $R = 0.969$ for nine observations. The data in parentheses are standard deviations.

a slope of −34 (±3) mV/pH unit (species **1**; Table I) and the current decreases; at pH less than about 8, the features lose both resolution and intensity. Most studies, to which the following results and discussion refer, were carried out at pH 12.9.

Under argon in the open-laboratory conditions, three additional weak peaks are generally seen, at −0.25 to −0.33 V (peak II, cathodic), −0.5 V (peak III), and −0.78 V (peak IV, cathodic) (Figure 3B). Their relative currents vary somewhat from experiment to experiment. Peaks II and IV are generally irreversible, showing no anodic counterpart, while peak III usually has an anodic counterpart at the same potential.

The current of peak II increases relative to that of peak I with decreasing concentration of the deposition DCB solution (Figure 3C) (equilibrium conditions). The electronic spectrum of the ClRh^{III}Pc/DCB solution does not obey Beer's law, with formation of aggregated species[25] being evident at concentrations as low as 1×10^{-4} M. Thus, deposition from more concentrated solutions likely deposits aggregated rather than monomeric species on the surface.

Under drybox (oxygen-free) conditions, in these equilibrium scans, peak II may appear weak and reversible, while peaks III and IV are very weak or indeed absent (Figure 3C).

(iii) Stability of Peak I (Experiments with ClRh^{III}TNPc (2)). The species giving rise to peak I is, as demonstrated below, a surface-bound dimeric rhodium tetraneopentoxyphthalocyanine which is not completely stable on the surface. If, after the equilibrium scan is established, the cyclic voltammogram is switched ~150 mV to either side of peak I, i.e. scanning repeatedly over peak I, the peak collapses over a few cycles and disappears, even though there are no other apparent redox processes within 150 mV of peak I. Thus surface-bound dimeric $[\text{RhTNPc}]_2$ is unstable upon polarizing over peak I.

To determine whether it is the Rh^{II}TNPc dimer (**3**) or the Rh^{III}TNPc dimer (**4**) which is unstable, an equilibrium scan was first established, and then the potential was held constant, 150 mV *negative* of peak I (i.e. with the Rh^{II}TNPc dimer (**3**) on the surface), for 5 min. A DPV scan then showed a decrease in the cathodic current of peak I of ~40%. Simiarly if an equilibrium surface is held just *positive* of peak I for only 0.5 min and then a DPV scan run, the cathodic DPV current is reduced by 70%. Thus, decomposition of the oxidized dimer $[\text{Rh}^{III}\text{TNPc}]_2$ (**4**) (which probably has bound hydroxide ions in the outer axial sites, i.e. is really (HO)Rh^{III}TNPc·TNPcRh^{III}(OH)) is fairly rapid, but decomposition of the $[\text{Rh}^{II}\text{TNPc}]_2$ species (**3**) is relatively slow.

Consistent with this observation, the anodic charge for peak I is always slightly greater than the cathodic charge. This is because there is some loss of dimeric species every time the electrode is polarized positive of the anodic component.

If a surface having been cycled over the potential corresponding to peak I is now polarized to negative potentials, increased reduction current is seen in the range −0.3 to −0.5 V (Figure 4c). Further, if the surface of **2** is polarized at 0 V for 30 s (Figure 4a,b), resulting in a loss of 70% of the charge of peak I, and is then polarized to −0.5 V and switched, 90% of the initial charge is recovered (Figure 4c,d).

It is interesting to observe that, with a brand new surface showing a strong peak V, it is necessary to cycle beyond −0.8 to

(25) Nevin, W. A.; Liu, W.; Lever, A. B. P. *Can. J. Chem.* **1986**, *65*, 855 and references therein.

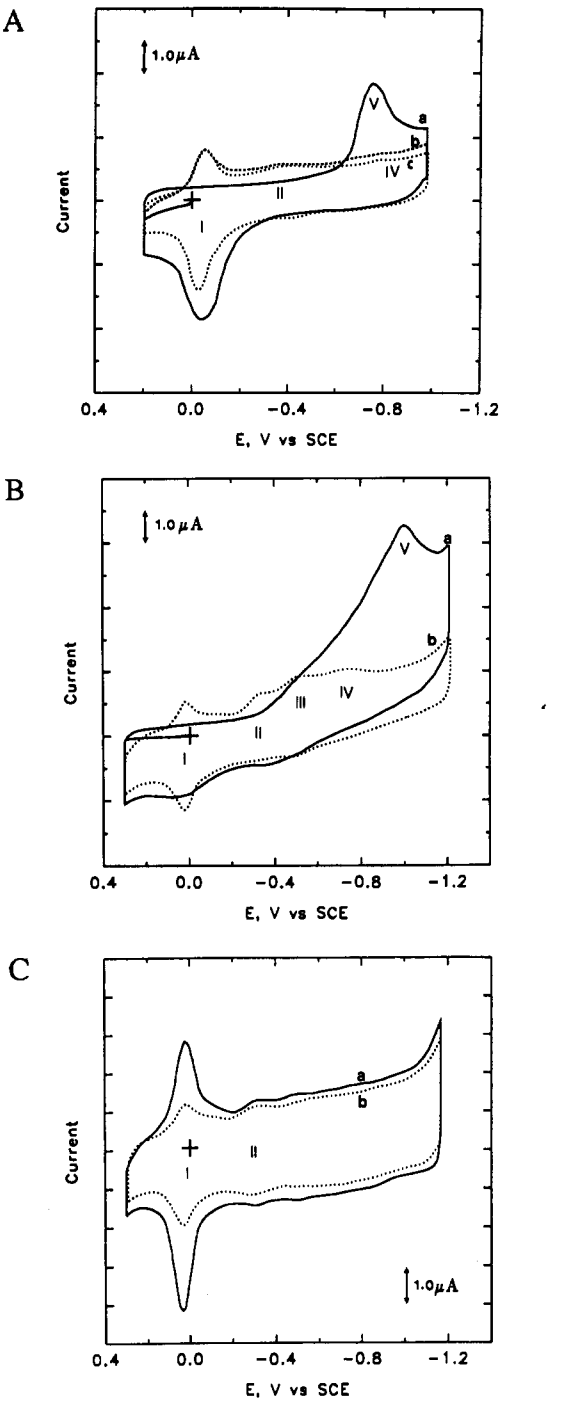

Figure 3. (A) Cyclic voltammograms for ClRhTNPc (**2**) on HOPG in 0.1 M KOH (scan rate 100 mV/s; drybox conditions): (a) first scan after adsorption, positive ongoing from 0 V; (b) second scan after adsorption; (c) equilibrium scan. The potentials and surface charges of the various peaks are as follows (peak, V, μC/cm^2): I, −0.05, 3.01; II, −0.35, 0.81; IV, −0.80, 0.16; V, −0.75, 8.38. The potentials remain constant from one experiment to another, but surface charges vary. Charges reported for this and subsequent figures are typical, and are rather approximate, given the uncertainty in assessing the charging current. (B) Cyclic voltammograms for ClRh^{III}Pc (**1**) on HOPG in 0.1 M KOH (scan rate 100 mV/s; argon degassed: (a) first scan after adsorption, positive ongoing from 0 V; (b) equilibrium scan. The potentials and surface charges of the various peaks are as follows (peak, V, μC/cm^2): I, 0.03, 1.41; II, −0.32, 0.48; III, −0.48, 0.63; IV, −0.72, 0.15; V, −0.96, 8.8. (C) Cyclic voltammograms for ClRh^{III}Pc (**1**) in 0.1 M KOH (scan rate 100 mV/s; drybox conditions): (a) concentration in deposition solution [ClRh^{III}Pc] = 1.73×10^{-4} M; (b) concentration in deposition solution [ClRh^{III}Pc] = 1.15×10^{-5} M. The potentials and surface charges of the various peaks are as follows (peak, V, μC/cm^2): Ia, 0.02, 6.2; Ib, 0.02, 1.9; IIa, −0.32, 0.44; IIb, −0.32, 0.43.

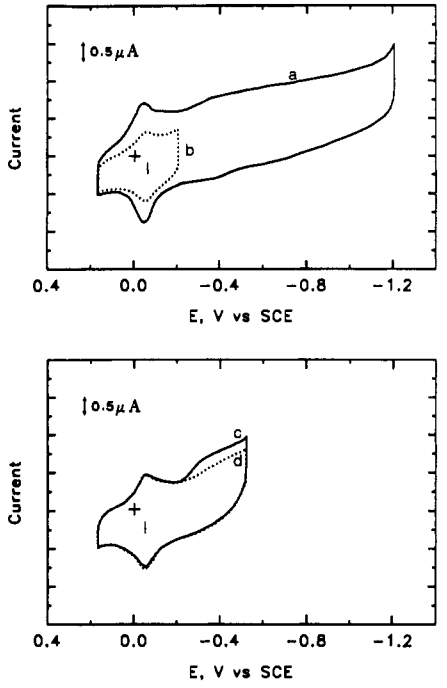

Figure 4. Cyclic voltammograms for ClRhTNPc (**2**) in 0.1 M KOH (argon degassed): (a) equilibrium scan, from +0.2 to −1.2 V; (b) scan from +0.2 to −0.2 V after polarizing the surface at zero potential for 30 s; (c) first scan following trace b, from +0.2 to −0.5 V; (d) second scan after trace b, from +0.2 to −0.5 V.

−1.0 V (beyond peak V) before there is significant growth of peak I. However, when an equilibrium surface with peak I has been produced and then polarized beyond 0 V, to cause loss of current intensity in peak I, it is only necessary to polarize the electrode to about −0.5 V to recover couple I.

Further, if a surface is polarized between about +0.2 V and −1.0 V, then, as the scan rate is decreased and the amount of time the surface remains as $[Rh^{III}TNPc]_2$ increases, the charge under peak II increases, at the expense of the charge under peak I. Data for this experiment are analyzed in Figure 5, as follows. Assume that at the highest scan rate, 150 mV/s, there is negligible decomposition of the dimer, since it exists as $[Rh^{III}TNPc]_2$ (**4**) for a very short period. Considering first the current, a line drawn between this 150 mV/s datum point and zero provides the theoretical dependence of current upon scan rate for no decomposition (recall that current is proportional to scan rate for a surface-bound species).[26] Then, observe that at lower scan rates the experimental points for peak I lie below the calculated line for no decomposition while those for peak II lie above it. Similarly, the charge under peak II is proportionately larger at low scan rates than at high scan rates, while the reverse is true for peak I. These charges reflect direct measurements of the ratio of "standing population" of the species responsible for peaks I and II and show that the dimeric species decomposes when polarized positive of peak I, to form the species displaying peak II. The total charge under these two peaks is constant, as is necessary (Figure 5B).

While, in principle, kinetic data could be extracted from this experiment, the uncertainty as to the residual (charging) current would lead to rather large errors in the data shown in Figure 5. The result is illustrative of the experiment undertaken and provides useful insight into surface behavior, but does not merit further analysis.

Note that the dimeric $[Rh^{III}Pc]_2$ species prepared from $ClRh^{III}Pc$, or directly from the bulk dimer solution (vide infra), is very much more stable than the corresponding $[Rh^{III}TNPc]_2$ species perhaps because the neopentoxy groups in the latter species interfere with the stabilization of the dimer. Cycling over peak I for $[RhPc]_2$ (±300 mV, 100 mV/s) leads to a loss of some 50%

(26) Shigehara, K.; Anson, F. C. *J. Phys. Chem.* **1982**, *86*, 2776.

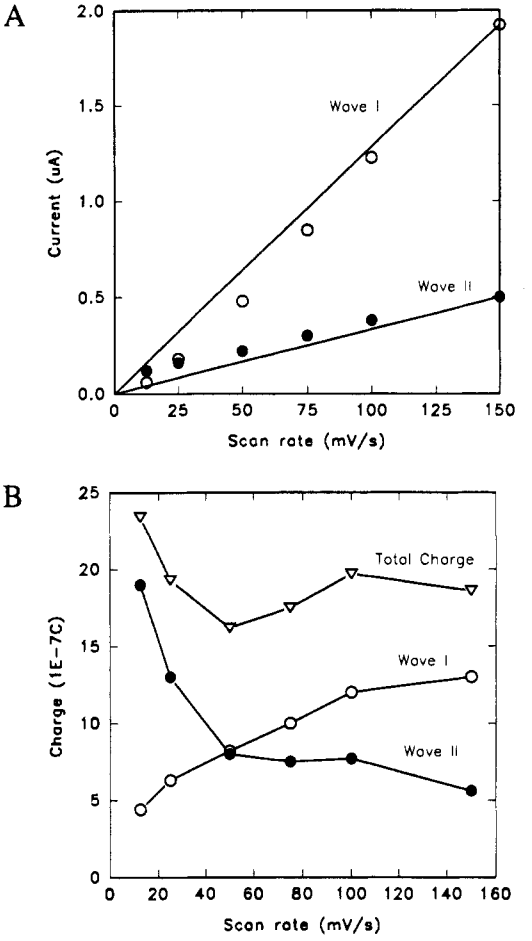

Figure 5. (A) Cathodic current of peaks I and II, species **2**, plotted against the scan rates for the surface in Figure 2. See text for significance of line. (B) Total cathodic peak charges for peaks I and II, species **2**, plotted vs scan rates, for the surface in Figure 2. See text for significance of line. The data are rather scattered due to the difficulty in estimating the residual currents, which must be subtracted from the observed data before plotting.

of the current only after about 10 min.

(iv) Surface Deposition from a Bulk Dimer Solution. Bulk electrolysis of a solution of $ClRh^{III}Pc$ in DMF at potentials negative of peak C (Figure 1) yields solutions whose electronic spectra (Figure 2) are consistent with the formation of the $[Rh^{II}Pc]_2$ dimeric species.

When an electrode is dipped into this solution for 0.5–1 h, a dimer surface is directly deposited. In contrast to the voltammetry discussed above, this premade dimer surface exhibits peak I on the first scan and exhibits no rapidly rising cathodic current negative of −0.5 V on the first scan.

There appear to be two slightly different dimer species on the surface, differing perhaps in their axially bound counterion or solvent. As initially formed in the fashion described above, one species exhibits an anodic peak at 0.15 V and its cathodic counterpart at 0.13 V vs SCE. In addition, there is a cathodic peak for the second species observed at 0.02 V vs SCE (with no anodic partner). If the surface is maintained for about 15 min and polarized at about 0.3 V, subsequent scans reveal only one dimer peak couple at 0.02 V, identical within experimental error to the species reported in section II.

Thus, deposition from the bulk dimer solution leads, after polarization of the resulting surface at 0.3 V, to the same surface as that generated from the bulk monomer solution.

(v) Introduction of Oxygen. Considering the data in Figure 6, the initial equilibrium surface (Figure 6a) is exposed to 0.01 mM oxygen and polarized around peak I. There is a fairly rapid loss of signal for peak I (Figure 6b). If this same surface in the 0.01 mM oxygenated solution is polarized out to −1.0 V, a new diffusion (cathodic) peak (as indicated by scan rate dependence),

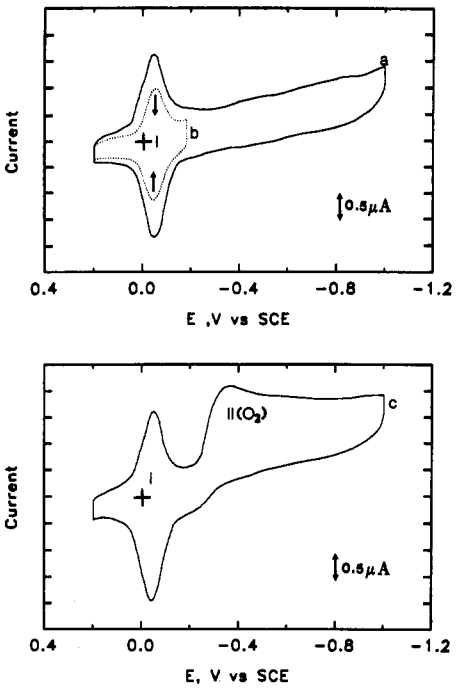

Figure 6. Cyclic voltammograms for ClRhTNPc (**2**) in 0.1 M KOH: (a) equilibrium scan, from +0.2 to −1.0 V, argon degassed; (b) scan from +0.2 to −0.2 V for 60 s after about 0.01 mM dioxygen is introduced into the cell; (c) second scan after trace b, from +0.2 to −1.0 V. Scan rate = 100 mV/s.

designated peak II(O_2), is seen at the same potential as peak II. Further, and most significantly, peak I is restored essentially quantitatively, but with the anodic component notably larger than the cathodic component. A similar experiment in a saturated oxygen environment (1 mM O_2) gave essentially the same results. Even under saturated oxygen conditions, scanning beyond −0.5 V regenerates peak I, though with somewhat less charge than the initial argon surface. The loss of peak I when polarizing is limited to ±150 mV of the peak I center, in a saturated oxygen environment, is more rapid than when cycling is undertaken under argon.

The peak potential for peak II(O_2) (in the presence of 0.01 mM O_2) shifts negatively about 45 mV with change in scan rate from 12.5 to 150 mV/s (species **1**), consistent with a relatively low rate constant for oxygen reduction. When the aqueous buffer solution is saturated with oxygen (ca. 1.1 mM),[27] a typical voltammogram for oxygen reduction on MPc/HOPG is obtained (Figure 7A), with E_p = −0.4 V vs SCE (at pH = 13) and a peak current of about 300–400 μA. The O_2 reduction peak potential is a function of pH, as expected,[15,19] shifting to more positive potentials with lower pH; however, because of the variability of the surface, peak potential data versus pH were somewhat scattered and are not further discussed.

(vi) RDE Experiments under an Oxygen Atmosphere. Figure 7B shows data collected with a rotating HOPG disk, using the ClRh^{III}Pc-modified equilibrium surface shown in Figure 3B. Using the Levich equation,[28] the number of electrons, n, involved in the reduction was 2.1–2.2, indicating a 2-electron reduction from oxygen to hydrogen peroxide.

However, if a surface was deliberately exposed to a small amount of oxygen during cycling to equilibrium, then, upon subsequent exposure to saturated oxygen, the rotating-disk study led to $n > 3$ electrons, though this was not invariably true.

The deliberate addition of some deoxygenated hydrogen peroxide to an argon equilibrium surface yielded an increase in the current of the anodic component of peak I, showing reoxidation

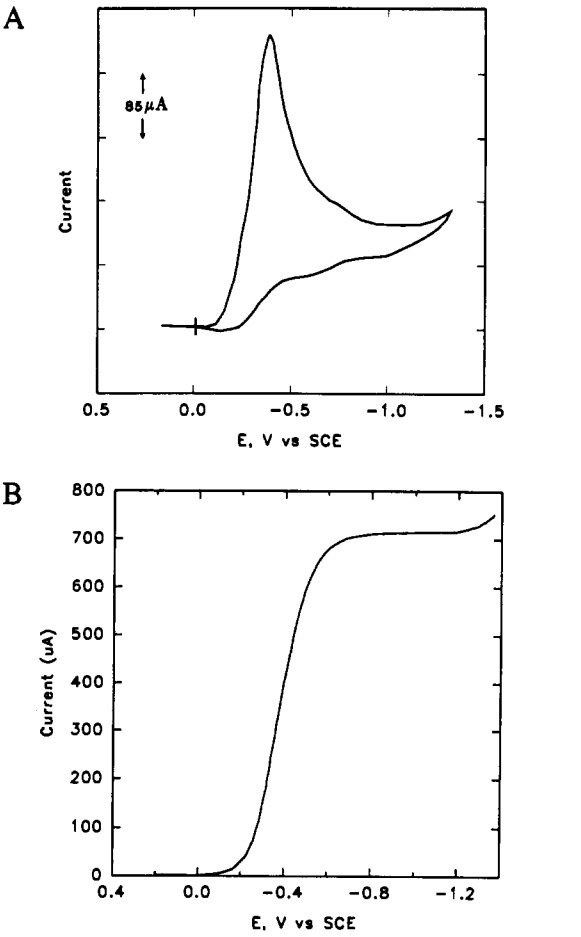

Figure 7. (A) Cyclic voltammogram for ClRh^{III}Pc (**1**) (layer adsorbed from DCE/5% ethanol solution on HOPG electrode; 0.1 M KOH; saturated with dioxygen; scan rate 100 mV/s). (B) Rotating disk electrode study of the surface in part A (400 rpm; scan rate 20 mV/s).

of hydrogen peroxide at that potential.

Discussion

Solution Electrochemistry. Kadish and co-workers have reported[29] an electrochemical study of the analogous ClRhTPP species (TPP = dianion of tetraphenylporphyrin). The results for ClRh^{III}Pc are very similar to those for ClRhTPP, as is immediately evident by comparing the solution voltammogram for ClRh^{III}Pc, shown in Figure 1, with the corresponding data for ClRhTPP (Figure 1, ref 29).

On the basis of the ClRhTPP analysis, and detailed experiments on ClRh^{III}Pc to be reported elsewhere,[24] the following conclusions concerning the solution voltammogram shown in Figure 1 can be drawn.

A bulk solution of ClRh^{III}Pc, in DMF, reduced at peak C forms a Rh^{II} derivative which, at ambient temperature, immediately dimerizes, forming a [Rh^{II}Pc]$_2$ species whose identity as a dimer is supported through spectroelectrochemical measurements (Figure 2) and analogy with the corresponding formation of a dimeric species upon reduction of ClRhTPP.[29]

This dimerization is suppressed at −72 °C, where a reversible monomeric Rh^{III}/Rh^{II} redox process is observed at −0.82 V. Peak D, at −1.42 V, represents the further reduction of this dimer species.

Peaks A and B are not observed unless the scan proceeds beyond a potential corresponding with peak C, and thus are dimer oxidation processes. These dimer reoxidation peaks (A and B) are missing in the −72 °C experiment because the dimer is not present under these conditions. Peak A corresponds to a reversible 2-electron oxidation forming [Rh^{III}Pc]$_2^{2+}$ (with charge likely com-

(27) Golovin, M. N.; Seymour, P.; Jayaraj, K.; Fu, Y.-S.; Lever, A. B. P. *Inorg. Chem.* **1990**, *29*, 1719.
(28) Levich, V. G. *Physicochemical Hydrodynamics*; Prentice-Hall: Englewood Cliffs, NJ, 1962.
(29) Kadish, K. M.; Yao, C. L.; Anderson, J. E.; Cocolios, P. *Inorg. Chem.* **1985**, *24*, 4515.

Scheme I

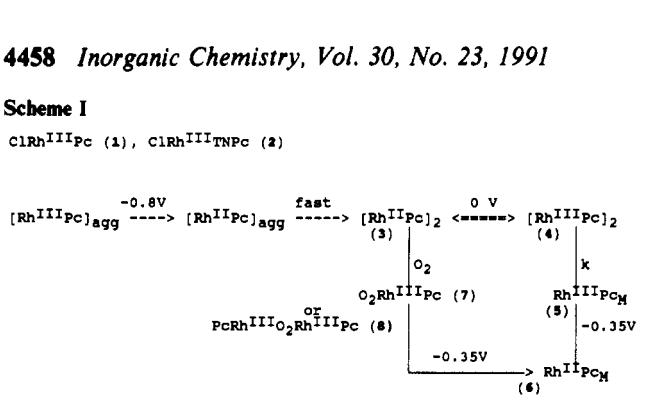

pensated by supporting electrolyte anions). Peak B is evidently associated with the formation of the dimeric species, but its identity is not clear.[31]

Surface Electrochemistry (Oxygen-Free Conditions). Peak I appears at essentially the same potential as observed for the 2-electron dimer redox process $[Rh^{III}Pc]_2/[Rh^{II}Pc]_2$ in solution, and the shift with pH is consistent with a 2-electron process. Further, this peak is the only peak observed (between +0.5 V and −1.0 V vs SCE) when deposition is carried out with bulk $[Rh^{II}Pc]_2$ dimer solution. Therefore, peak I is a 2-electron Rh^{III}/Rh^{II} couple for a dimeric $[RhPc]_2$ species; see Scheme I.

The surface voltammetry can be understood in terms of the following model. When freshly deposited, $ClRh^{III}Pc$ gathers in randomly distributed, poorly organized, and likely aggregated species, interacting fairly weakly with the electrode surface. Assumptions have been made[30] that, on highly oriented pyrolytic graphite, phthalocyanines will adsorb by interaction of the macrocycle π-clouds with those of the graphite lattice and thus that the macrocycle lies flat on the graphite. However, simple microscopic examination of a supposedly "mirror" graphite surface shows many imperfections which can act as nucleating sites for the catalyst. Formation of "clumps" on the electrode surface will be further facilitated if the catalyst is already aggregated.

These poorly organized species give rise to the reduction current seen in the initial voltammogram between −0.5 and −1.0 V, especially to peak V near −0.8 to −0.9 V (Figure 3A,C). This potential corresponds to that observed (−0.82 V) for the quasi-reversible mononuclear $ClRh^{III}Pc/Rh^{II}Pc$ process in DMF/TBAP at −72 °C[24] and is similarly assigned here to reduction of $ClRh^{III}Pc$ to $Rh^{II}Pc$. Because of the close association of the $Rh^{II}Pc$ species in these aggregates, the $Rh^{II}Pc$ fragments rapidly dimerize, giving rise to peak I, and hence peak V is irreversible.

The species $[Rh^{II}Pc]_2$ (**3**) is somewhat unstable when oxidized to the rhodium(III) dimer, $[Rh^{III}Pc]_2^{2+}$ (**4**), splitting apart slowly into mononuclear rhodium(III) phthalocyanine fragments (**5**). When cycling is carried out around 0 V, the resulting $[Rh^{III}Pc]^+$ fragments (**5**) are not reduced and therefore cannot redimerize, and couple I collapses completely. However, when such a surface is polarized more negatively, current is increased in the region beyond about −0.35 V (Figure 4c) because of the reduction of these rhodium(III) phthalocyanine fragments (**5**) to mononuclear $Rh^{II}Pc$ (**6**) species which rapidly redimerize, so that when cycling is extended negative of the potential corresponding to peak II, the dimer couple, I, is restored essentially quantitatively (see Figure 4c,d). Thus, peak II is associated with the Rh^{III}/Rh^{II} couple of a mononuclear rhodium phthalocyanine species.

The rhodium(II) dimeric species (**3**) decomposes slowly on the surface. It is probable that, in fact, this species is intrinsically stable on the surface, as it is in solution, but that it is slowly converted to mononuclear species by reaction with trace oxygen or other reactive impurities. The amount of material on the surface of the electrode is of the order of 40 fmol, so that very little reactive impurity is needed to destroy it.

Consideration of the charge under dimer peak I, and assuming a 2-electron process, gave a coverage (over a series of experiments) in the range of 20–40% of a monolayer of dimers; we only very rarely observed greater coverage than this. Under drybox conditions, the very weak peak II corresponds to about 0.5% surface coverage. Thus, much of the surface apparently remains uncovered. The apparent reversibility of peak II under drybox conditions may then arise through mononuclear $Rh^{II}Pc$ (**6**) species which are too far apart to dimerize.

Peak II at −0.35 to −0.45 V, associated with the reduction of mononuclear $Rh^{III}Pc$, is positive of the corresponding peak in solution at −0.82 V (low-temperature reversible datum). Therefore, surface-bound mononuclear rhodium phthalocyanine (**6**) is stabilized in the divalent state relative to the solution species[31] probably because of the interaction of the odd electron in the d_{z^2} orbital with the graphite surface; i.e., rhodium(II) is probably bound chemically to the surface. A fresh surface containing poorly organized $ClRh^{III}Pc$ which is not, in its reduced $Rh^{II}Pc$ state, chemically bound to the graphite surface will show a redox potential near −0.8 V (peak V).

Dimerization of the $Rh^{II}Pc$ species (slowly upon cycling with $ClRh^{III}Pc$ (**1**) and rapidly with ClRhTNPc (**2**)) causes binding to the surface such that peak V is lost. Once formed, this bound dinuclear $[Rh^{II}Pc]_2$ species (**3**) oxidizes at a potential positive of peak I to $[Rh^{III}Pc]_2$ (**4**), which subsequently decomposes to mononuclear **5**, which remains bound to the graphite surface, albeit perhaps weakly. This $[Rh^{III}Pc]^+$ species (**5**), then, can be reduced in the range −0.25 to −0.4 V, peak II, to produce $Rh^{II}Pc$ (**6**) bound to the graphite surface; this can readily dimerize. The spread of potentials likely reflects possible alternate axial ligands, including water, supporting electrolyte anion, and oxygen (vide infra). Indeed, the more negative potential of peak V, relative to peak II, in the initial scan is partially a consequence of the bound chloride ion which is lost during reduction to $Rh^{II}Pc$ and which would stabilize rhodium(III). The possibility that the axially bound chloride ion is the primary reason for the difference in these potentials and that binding to the graphite surface is not a factor seems improbable on the basis of the fact that the addition of chloride ion (0.1 M) to the electrolyte solution (pH 12.9) does not cause peak V to be retained beyond the first scan.

Peak IV is seen weakly on some equilibrium surfaces but does not always occur. That it was frequently (but not always) absent from the drybox-collected data suggests that it might be assigned to another oxygen adduct or perhaps the μ-oxygen-bridged species $PcRh^{III}ORh^{III}Pc$. μ-Oxo-bridged phthalocyanines and porphyrins have reduction potentials significantly negative of the corresponding process in the mononuclear species;[32] thus, the observation of peak IV negative of peak II is consistent with this assignment.

Surface Electrochemistry under Oxygen. Peak $II(O_2)$ is clearly an oxygen reduction peak occurring at the same potential as the $Rh^{III}Pc/Rh^{II}Pc$ monomeric couple (peak II under argon) (Figure 6). The increase in current in the anodic component of peak I is due to hydrogen peroxide reoxidation occurring at a potential the same as that of the dimer species oxidation and corresponding roughly with the thermodynamic oxidation potential at pH 12.9. Some catalytic reoxidation of hydrogen peroxide may be involved.[33]

Dimer species $[Rh^{II}Pc]_2$ (**3**) reacts with oxygen, but slowly, because (a) peak I is diminished but not lost in the presence of a low level of oxygen (Figure 6), (b) cycling just negative of peak I, under oxygen, causes a faster collapse of peak I than cycling under argon, (c) peak I can be regenerated if the oxygenated surface is polarized more negative than peak $II(O_2)$ (ca. −0.5 V) (Figure 4), and (d) cathodic oxygen reduction occurs ~200–350 mV negative of couple I (Figure 6).

Note that during a positive ongoing scan, while the potential is in the range from about −0.2 V (positive of peak II) to 0 V (negative of peak I), $[Rh^{II}Pc]_2$ (**3**) will exist on the surface and will be oxidized by oxygen. If such oxidation were very rapid, peak I would disappear; instead, it is diminished relative to the situation under an argon atmosphere. If one were to argue that

(30) Janda, P.; Kobayashi, N.; Auburn, P. R.; Lam, H.; Leznoff, C. C.; Lever, A. B. P. *Can. J. Chem.* **1989**, *67*, 1109.

(31) Ni, C.-L.; Anson, F. C. *Inorg. Chem.* **1985**, *24*, 4754.

(32) Minor, P. C.; Lever, A. B. P. *Inorg. Chem.* **1983**, *22*, 826.

(33) Elzing, A.; Van Der Putten, A.; Visscher, W.; Barendrecht, E. *J. Electroanal. Chem. Interfacial Electrochem.* **1986**, *200*, 313.

only mononuclear, and not dinuclear, rhodium phthalocyanine surface species react with oxygen, then the magnitude of peak I should be independent of whether the atmosphere is argon or oxygen.

Dimeric rhodium(II) porphyrins react with oxygen to form both monomeric superoxorhodium(III) and bridged dinuclear peroxorhodium(III) porphyrin species.[34-38] Iridium octaethylporphyrin is also believed to form a μ-peroxo dimeric species.[12] Therefore, analogous species, viz. $(O_2)Rh^{III}Pc$ (7) and $PcRh^{III}O_2Rh^{III}Pc$ (8), are also likely found on the phthalocyanine surface. It has also previously been demonstrated[38] that (O_2)-$Rh^{III}TPP$ is irreversibly reduced, to a dimeric $[Rh^{II}TPP]_2$ species, at a potential slightly less negative than that of $(Cl)(Me_2NH)$-$Rh^{III}TPP$; thus, oxygenated rhodium(III) phthalocyanine may be reduced at a potential close to that of some unoxygenated mononuclear rhodium(III) phthalocyanine species.

During the cycling to equilibrium in the argon-degassed experiment where trace oxygen is probably present, some of the rhodium species will be trapped as oxygen adducts. The increased current near −0.25 to −0.4 V (peak II under argon, Figure 3B) then arises from a superimposition of (a) the reduction of $Rh^{III}Pc$ monomer species (5) generated through decomposition of 4, (b) the reduction of oxygen adducts, 7 and/or 8, and (c) some very small current due to reduction of diffusing trace oxygen. Peak III, which is usually absent in data collected under drybox conditions, likely arises from an oxygen adduct differing from that responsible for current near peak II.

The oxygen reduction process occurring at peak II may be represented by the series of reactions

$$[Rh^{II}Pc]_2 + 2O_2 \rightarrow 2[(O_2^-)Rh^{III}Pc] \quad (1)$$

$$[(O_2^-)Rh^{III}Pc] + 2e^- + H^+ \rightarrow HO_2^- + [Rh^{II}Pc] \quad (2)$$

$$2[Rh^{II}Pc] \rightarrow [Rh^{II}Pc]_2 \quad (3)$$

where the oxygen adduct is assumed to be mononuclear 7, but might readily be dinuclear 8, without affecting the overall argument. The recovery of peak I upon scanning under oxygen negatively of −0.5 V is explained through eqs 2 and 3; i.e., the reduced oxygen adduct will immediately redimerize (cf. the RhTPP system[38]).

RDE experiments yield higher n values if the initial surface has some contact with oxygen than if it does not. The formation of an equilibrium surface in the presence of a small amount of oxygen, followed by the oxygen electrocatalysis study, might yield a different distribution of oxygen adducts on the surface than if the initial surface is generated oxygen-free. One might then speculate that mononuclear 7 acts as a 2-electron reductant to give hydrogen peroxide, while dinuclear 8 acts as a 4-electron reductant to give water. However, it has proved very difficult to control these surfaces to routinely obtain n values in excess of 3 electrons.

Summary

The processes seen on the rhodium phthalocyanine modified HOPG electrode may be summarized as follows (also see Scheme I): peak I, reversible dimeric RhPc species redox, 3 ↔ 4; peak II, mononuclear RhPc species redox, 5 ↔ 6; peak II(O_2), reduction of diffusing oxygen possibly via a $Rh^{III}Pc$ oxygen adduct species; peak III, oxygen adduct redox process; peak IV, possible reduction of $PcRh^{III}ORh^{III}Pc$; peak V, reduction of $ClRh^{III}Pc$ species unbound to the graphite surface.

The rhodium phthalocyanine surface exhibits some unusual behavior, with the dynamic interplay between mononuclear and dinuclear species on the surface being especially noteworthy. By appropriate control of the polarization potential, it would clearly be possible to "hold" any one of several different RhPc species on the surface. Our initial objective to demonstrate a 4-electron reduction pathway for oxygen met with only limited success. However, the chemistry developed offers some important future avenues, such as the possibility that these equilibria can be coupled to other multielectron electrocatalytic processes, in addition to that with oxygen.

Acknowledgment. We are indebted to Drs. K. Kandil and K. Jayaraj for experimental assistance, to Dr. Pavel Janda for useful discussions, and the Natural Sciences and Engineering Research Council (Ottawa) and the Office of Naval Research (Washington) for financial assistance. Our thanks are also expressed to Johnson-Matthey for the loan of $RhCl_3$ and to Union Carbide for the HOPG.

Registry No. 1, 14285-57-5; 2, 136658-96-3; RhPc, 37099-31-3; RhTNPc, 136658-97-4; $[RhPc]_2^{2+}$, 136658-98-5; $[RhTNPc]_2^{2+}$, 136658-99-6; $[RhPc]_2$, 136659-00-2; $[RhTNPc]_2$, 136675-77-9; O_2, 7782-44-7; H_2O_2, 7722-84-1; H_2O, 7732-18-5; graphite, 7782-42-5.

(34) Gillard, R. D.; Heaton, B. T.; Vaughn, D. H. *J. Chem. Soc. A* **1970**, 3126.
(35) Addison, A. W.; Gillard, R. D. *J. Chem. Soc. A* **1970**, 2523.
(36) Ogoshi, H.; Setsune, J.; Yoshida, Z. *J. Am. Chem. Soc.* **1977**, *99*, 3869.
(37) Wayland, B. B.; Newman, A. R. *J. Am. Chem. Soc.* **1979**, *101*, 6472. Wayland, B. B.; Newman, A. R. *Inorg. Chem.* **1981**, *20*, 3093.
(38) Anderson, J. E.; Yao, C.-L.; Kadish, K. M. *Inorg. Chem.* **1986**, *25*, 3224.